

Shapiro Step Response in the Coherent Josephson Flux Flow State of $\text{Bi}_2\text{Sr}_2\text{CaCu}_2\text{O}_{8+\delta}$

Yu. I. Latyshev,^{1,2} M. B. Gaifullin,³ T. Yamashita,¹ M. Machida,⁴ and Yuji Matsuda³

¹Research Institute of Electrical Communications, Tohoku University, 2-1-1, Katahira, Aoba-ku, Sendai 980-8577, Japan

²Institute of Radio-Engineering and Electronics, Russian Academy of Sciences, Mokhovaya 11, Moscow 103907, Russia

³Institute for Solid State Physics, University of Tokyo, Kashiwanoha 5-1-5, Kashiwa, Chiba 277-8581, Japan

⁴Center for Promotion of Computational Science and Engineering, Japan Atomic Energy Research Institute, 2-2-54 Nakameguro, Meguro-ku, Tokyo 153-0061, Japan

(Received 24 May 2001; published 27 November 2001)

We report the first observation of Shapiro steps in the Josephson flux flow state of $\text{Bi}_2\text{Sr}_2\text{CaCu}_2\text{O}_{8+\delta}$ stacked junctions. When the junction is irradiated at microwave frequencies in a strong parallel magnetic field ($H \geq 1$ T), a steep increase of the current is observed in the dc current-voltage characteristics when the external microwave frequency and the Josephson frequency are harmonically related. The existence of Shapiro steps in the Josephson flux flow state is strong evidence of coherent motion of the Josephson vortex lattice through the whole thickness of the stack.

DOI: 10.1103/PhysRevLett.87.247007

PACS numbers: 74.50.+r, 74.25.Nf, 74.60.Ge, 74.72.Hs

Highly anisotropic high- T_c superconductors (HTSC), such as $\text{Bi}_2\text{Sr}_2\text{CaCu}_2\text{O}_{8+\delta}$, can be considered as stacks of superconducting CuO_2 layers coupled by the Josephson interaction [1]. Several properties which have never been observed in single Josephson junctions made from conventional low- T_c materials have been found, which are associated with the multilayer structure and with the atomic thickness of the superconducting layers. In particular, the vortex phase diagram and the related electromagnetic properties of HTSC in the presence of a strong magnetic field parallel to the layers have been the subject of recent intense experimental and theoretical studies [2–9]. For instance, the phase transition of Josephson vortices with different structure is one of the central topics of the physics of vortex matter [2,3]. In particular, the phase diagram of moving Josephson vortices attracts much attention because the strong coupling between the vortex motion and the transverse Josephson plasma excitation mode gives rise to novel vortex phases which have never been realized in a system of Abrikosov vortices [5–7]. Moreover, a collective electromagnetic excitation associated with moving Josephson vortices has attracted much attention because it is closely related to strong coherent electromagnetic wave emission which is very important for the practical applications of HTSC [6,10].

The dynamical properties of Josephson vortices have not been as well studied as static properties, which have been probed by several techniques such as magnetic susceptibility, neutron diffraction, and SQUID magnetometer spectroscopy. The main reason for this is that the dynamical properties have been investigated only by the c -axis dc resistivity caused by Josephson flux flow. The remarkable feature of the current-voltage (I - V) characteristics in the $\text{Bi}_2\text{Sr}_2\text{CaCu}_2\text{O}_{8+\delta}$ junction stack is multiple branches of the flux flow resistivity [11,12]. This branched structure has been discussed in the light of resonant modes that appear when the velocity of the Josephson lattice matches the velocity of the transverse plasma wave, similar to the

Eck step in a single Josephson junction [6,13–15]. However, the detailed dynamical structure of the vortices has been a controversial issue. In fact, even the lowest mode of the vortex propagation is not well understood. Recent numerical studies have revealed a very rich dynamical evolution of moving Josephson vortex structures, which include disordered structure, triangular lattice, square lattice, and dynamical phase separation of the different lattices [5–7]. The situation therefore strongly confronts us with the need for a powerful new probe of the dynamical properties of Josephson vortices. In this Letter, we report measurements of the microwave response in the I - V characteristics of $\text{Bi}_2\text{Sr}_2\text{CaCu}_2\text{O}_{8+\delta}$ stacked junctions in a strong parallel magnetic field. We observed an anomalous behavior in the lowest Josephson flux flow branch in the I - V characteristics, which can be attributed to Shapiro steps. We show that the observation of Shapiro steps in the flux flow state provides important information about the vortex dynamics.

Stacked intrinsic Josephson junctions were fabricated by double-sided processing of high quality $\text{Bi}_2\text{Sr}_2\text{CaCu}_2\text{O}_{8+\delta}$ ($T_c = 80$ K) whiskers by using a focusing ion beam technique [16]. The inset of Fig. 1 shows schematically the arrangement of the junctions. The length of the junction is $L = 30 \mu\text{m}$ with a width of $W = 2.0 \mu\text{m}$. The oxygen doping level estimated from c -axis resistivity was $\delta \sim 0.25$, indicating the slightly overdoped regime. The critical current j_c at 4.2 K in the absence of magnetic field was approximately $(1-2) \times 10^3 \text{ A/cm}^2$. External microwaves with a maximum incident power of 35 mW at the frequencies ranging from 45 to 142 GHz were applied from the backward-wave oscillators. The sample was mounted on the substrate which was placed at the center of the rectangular waveguides. The microwaves were applied to the junction with the electric component \mathbf{E}_{ac} along the c axis. The I - V characteristics were measured at several tenths of Hz using a low noise oscilloscope. The magnetic field was applied parallel to the layers within

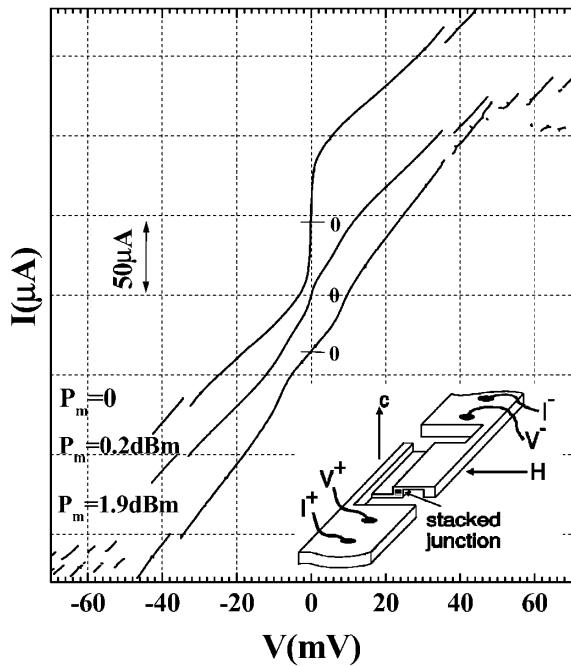


FIG. 1. I - V characteristics of the stacked intrinsic Josephson junction with and without microwave irradiation in a parallel field of 2.25 T at 6.3 K. The applied microwave frequency is 75.0 GHz. For clarity, the zero levels of the three curves are vertically shifted. Inset: Schematic arrangement of the stacked intrinsic Josephson junction fabricated by double sized processing of $\text{Bi}_2\text{Sr}_2\text{CaCu}_2\text{O}_{8+\delta}$ whiskers using the focusing ion beam technique.

0.01° and perpendicular to the long dimension L by split pair superconducting magnets.

In zero field, the I - V characteristics are typical of multi-layer Josephson junctions; the junctions have highly hysteretic I - V characteristics and the almost equally spaced branches appear in the resistive state. The total number of Josephson junctions N , estimated from the number of branches, is $N = 60 \pm 3$. Figure 1 depicts the I - V characteristics in the parallel field of 2.25 T at 6.3 K. In the absence of microwave irradiation ($P_m = 0$), the critical current is strongly suppressed to $\sim 1/30$ of j_c at $H = 0$. The linear slope with slight upturn in the I - V characteristics at finite voltage evidences the Josephson flux flow state. The multiple Josephson flux flow branches appear above 36 mV as discrete jumps in the current as the voltage is varied, similar to Ref. [11]. The I - V characteristics are changed dramatically when the junction is irradiated with microwave radiation of frequency $\omega/2\pi = 75.0$ GHz.

A striking feature is the appearance of anomalous structure in the I - V characteristics in the first branch near $V = 8$ mV, when the current increases more steeply than below and above this voltage. In Fig. 2 we plot dI/dV vs V under microwave radiation with various powers ($\omega/2\pi = 90.4$ GHz) in parallel field of 2.4 T at $T = 7.4$ K. The anomalous behavior in the current can be clearly seen. The first ($n = 0$), second ($n = 1$), third ($n = 2$), and fourth ($n = 3$) peaks appear at $V_0 = 0$ mV,

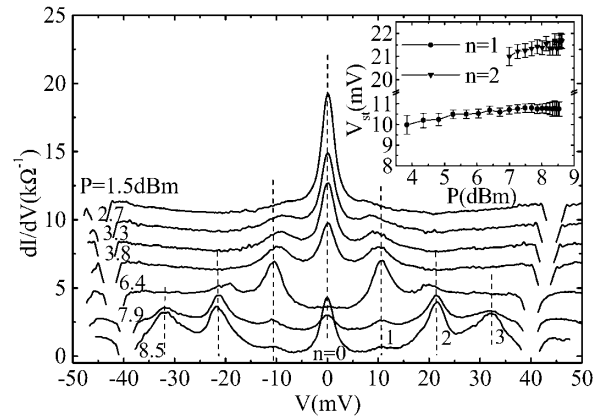


FIG. 2. dI/dV as a function of bias voltage V in microwave radiation with various powers ($\omega/2\pi = 90.4$ GHz) in parallel field of 2.37 T at $T = 7.4$ K. The broken lines represent the first ($n = 0$), second ($n = 1$), third ($n = 2$), and fourth ($n = 3$) peaks. Discontinuities near 40 mV in both polarities correspond to the branch switching. For details see the text. Inset: The microwave power dependence of V_1 and V_2 .

$V_1 = 10.7 \pm 0.2$ mV, $V_2 = 21.4 \pm 0.2$ mV, and $V_3 = 32.1 \pm 0.3$ mV, respectively. It is found that V_1 , V_2 , and V_3 are in the proportional relations; $V_2 = 2V_1$ and $V_3 = 3V_1$. Figure 3(a) shows the frequency dependencies of V_1 and V_2 in fixed parallel field of 2.25 T. It is obvious from Fig. 3(a) that both V_1 and V_2 are exactly proportional to the external microwave frequency. Figure 3(b) shows the field dependence of V_1 at a fixed frequency of 90.4 GHz. V_1 is independent of the external magnetic field. At $H = 1$ T, the maximum flux flow voltage of the first branch V_{ff}^m coincides with V_1 , below which V_1 cannot be identified. Figures 4(a)–4(c) show the magnitude of the change of the current ΔI_n at each step obtained from $(dI/dV)\Delta V$ at V_0 , V_1 , V_2 , and V_3 as a function of $\sqrt{P_m}$. Here ΔV is the voltage width where the anomalous increase of I is observed, which is determined from the

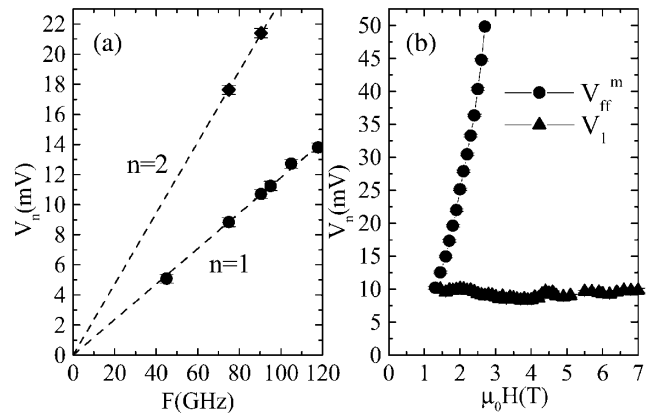


FIG. 3. (a) Microwave frequency dependence of V_1 and V_2 in a parallel field of 2.37 T. Dashed lines represent the proportional relation. (b) Field dependence of V_1 at a fixed frequency of 90.4 GHz. V_{ff}^m is the maximum flux flow voltage at the first branch.

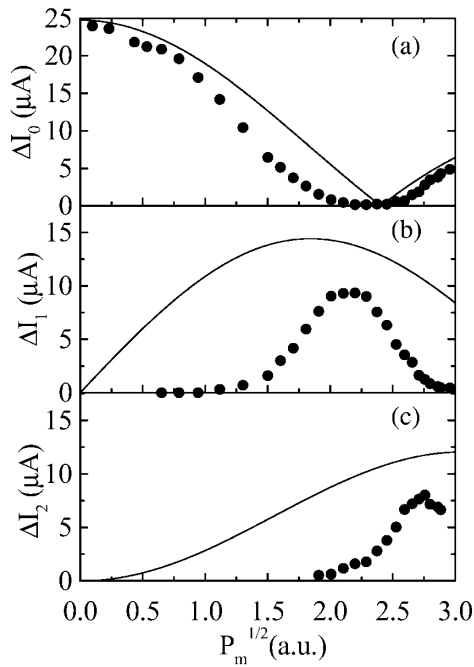


FIG. 4. Magnitude of the change of the current ΔI_n normalized by the critical current I_c at (a) $V = 0$ ($n = 0$), (b) V_1 ($n = 1$), and (c) V_2 ($n = 2$) as a function of the $\sqrt{P_m}$ ($\omega/2\pi = 90.4$ GHz) at 7.4 K in parallel field of 2.37 T. Solid lines represent the result of theoretical calculations of $\Delta I/I_c$ by Eq. (2). For details, see the text.

dI/dV vs V curve. We find that the amplitude of ΔI_n at each peak ($n = 0, 1, 2$, and 3) is an oscillatory function of the microwave power. The peaks in dI/dV are observed in fields ranging from 1 to 7 T up to $T = 75$ K. The same results were obtained in the junctions with different size. The following summarizes the salient features of the

anomalous increase of the current, which can be identified by the peak in the dI/dV vs V curve, observed in the first flux flow branch: (I) The peaks in dI/dV appear when the external microwave frequency and the Josephson frequency are harmonically related. (II) The amplitude of ΔI_n oscillates as a function of the amplitude of the microwave-drive voltage. (III) The position of the peak depends neither on the external magnetic field nor on the microwave power. These results lead us to conclude that the steep increase of the current which is recognized by the peaks in dI/dV can be attributed to *Shapiro steps in the flux flow state*, which occurs when there is interference between the ac Josephson effect and the microwave frequency. We will show that this observation provides several important pieces of information concerning the Josephson vortex dynamics. We now consider the Shapiro step in the presence of Josephson vortices, assuming the voltage bias case for simplicity. Neglecting the charge coupling term discussed in Ref. [4], the Josephson relation is written as $\partial P_{\ell,\ell+1}/\partial t = (2e/\hbar)V_{\ell,\ell+1}$, where $P_{\ell,\ell+1}$ and $V_{\ell,\ell+1}$ are, respectively, the gauge invariant phase difference and the voltage between ℓ th and $\ell + 1$ -th layers. When the microwave ac voltage is applied to a dc voltage-biased Josephson junction, $V = V_{dc} + V_{ac} \cos \omega t$, the phase difference along the spatial interval at time t can be written as

$$P_{\ell,\ell+1} = \gamma_{\ell,\ell+1} + \omega_J t + \alpha \sin \omega t + \varphi_0, \quad (1)$$

where $\gamma_{\ell,\ell+1} = \frac{2eDH}{\hbar c}x + Q_{\ell,\ell+1}$, $\omega_J = 2eV_{dc}/\hbar$, $\alpha = 2eV_{ac}/\hbar\omega$, D is the thickness of the insulating layers, and φ_0 is an arbitrary phase. Here, it is noted that $\gamma_{\ell,\ell+1}$ including $Q_{\ell,\ell+1}$ should be given by solving the coupled sine-Gordon equation. Then the resulting Josephson current in the junction is

$$\begin{aligned} I(t) &= W \int_0^L dx j_c \sin\{\gamma_{\ell,\ell+1}(x) + \omega_J t + \alpha \sin \omega t + \varphi_0\} \\ &= W \int_0^L dx j_c \left[J_0(\alpha) \sin\{\gamma_{\ell,\ell+1}(x) + \varphi_0 + \omega_J t\} + \sum_{n=1}^{\infty} J_n(\alpha) \left[\sin\{(\omega_J + n\omega)t + \gamma_{\ell,\ell+1}(x) + \varphi_0\} \right. \right. \\ &\quad \left. \left. + (-1)^n \sin\{(\omega_J - n\omega)t + \gamma_{\ell,\ell+1}(x) + \varphi_0\} \right] \right] \end{aligned} \quad (2)$$

where J_n are Bessel functions of the first kind of integer order. If we vary ω_J (by sweeping V_{dc}) such that the condition $\omega_J = \pm n\omega$ is met, then the time dependence associated with this term, having the amplitude $J_n(\alpha)$ and phase φ_0 , gives rise to the anomaly in the I - V characteristics. Thus the harmonical relation between V_{dc} and ω (Property I, discussed above) is consistent with Eq. (2). Moreover, since $J_n(\alpha)$ are oscillatory functions of α , the oscillatory behavior of ΔI_n (Property II) depicted in Figs. 4(a)–4(c) is consistent with Eq. (2). As we will show later, observed ΔI_n are quantitatively consistent with the numerical calculation.

We now discuss the implications of the present results. The Shapiro step observed in the Josephson flux flow state is markedly different from that of the conventional Shapiro step in zero field in two aspects. First, the dc voltage appears as a result of the quasiparticle dissipation due to Josephson flux flow in the present case, while it arises from the quasiparticle dissipation due to the uniform phase oscillation in the conventional case. Therefore the dc voltages of the Shapiro steps are closely related to Josephson vortex dynamics. The voltage of the Shapiro step at $n = 1$ is given as $V_{dc} = N^*(\hbar\omega/2e)$ where N^* is the number of

layers with the same speed of Josephson vortices. If the Josephson vortices move at different speeds in some layers, N^* is smaller than N , because moving vortices with different speed generate different voltages. $V_{dc} = 10.7$ mV at $\omega = 90.4$ GHz yields $N^* = 57$, which agrees with the number of the layers determined from the branched structure in zero field. This fact demonstrates that each junction generates the same voltage; *the Josephson vortices move at the same speed over the whole thickness of the stack.* Second, and more importantly, Eq. (2) contains the factor,

$$C = \int_0^L dx \sin\{\gamma_{\ell,\ell+1}(x) + \varphi_0\}, \quad (3)$$

which is absent in the conventional Shapiro step and represents the magnitude of the spatial coherence of the Josephson vortices. Thus the observation of Shapiro steps indicates that *a high degree of regularity of the moving Josephson vortices both parallel and perpendicular to the layers is achieved*, because if the vortex lattice is strongly deformed, the C factor should be strongly reduced from that of the periodic structure.

We finally show the results of the numerical calculation of ΔI_n in accordance with Eq. (2) assuming the coherent flux flow states. The present experiment is neither current biased nor voltage biased. In the calculation, we assumed voltage biased. In order to obtain $\gamma_{\ell,\ell+1}(x)$ in flux flow states, we performed numerical calculations on the damped coupled sine-Gordon equation given by $\gamma \frac{\partial \gamma_{\ell,\ell+1}}{\partial t} = -\frac{\delta F}{\delta \gamma_{\ell,\ell+1}}$, where F is free energy of intrinsic Josephson junction systems [17], and γ is a relaxation time in the steady flow states. The vortex lattice is slowly driven along the ab plane direction and the change of the total Josephson current with the flux flow is calculated by inserting $\gamma_{\ell,\ell+1}(x)$ in the steady states into Eq. (2). Thus, we can evaluate the total Josephson current variation in triangular lattice flow states as $\Delta I_n = I_{\max,n} - I_{\min,n}$, where $I_{\max,n}$ and $I_{\min,n}$ are the maximum and the minimum current calculated by Eq. (2), respectively. The obtained results are plotted in Figs. 4(a)–4(c) by the solid lines. The oscillatory behavior of ΔI_n is consistent with the data. Especially, for $n = 0$, the calculated $\Delta I_0/I_c$ coincides well with the data. The discrepancy of $\Delta I_n/I_c$ for $n = 1$ and 2 may be attributed to the assumption of the voltage biased. Thus, $\Delta I_n/I_c$ obtained by the numerical calculation well reproduce the data and reinforce our conclusion of the Shapiro step under the coherent vortex motion. Property III indicates that the Josephson vortices move at the same speed keeping the high regularity which is enough to observe the Shapiro steps along most of the first branch, at least above $H = 1$ T. This fact implies that the strong inductive coupling between Josephson vortices in the different layers plays an important role in the dynamical properties. Until now, Shapiro steps in Josephson junctions have been discussed only in the absence of magnetic field. To our knowledge, this is the first observation of

the Shapiro step in the presence of moving Josephson vortices. In the ordinary multilayer Josephson junctions, the Shapiro step response has never been observed in the flux flow regime. We believe that in such junctions the inductive coupling is not strong enough to give rise to the coherent motion of the Josephson vortices in the whole stacks.

We finally comment on the electromagnetic radiation from the intrinsic junction. From the present results of the microwave absorption, we can expect to obtain a very powerful microwave emission. According to a rough calculation, the emitted microwave power P_W estimated from the relation $P_W \sim \Delta IV_1$ gives a value as large as $P_W \sim 10^{-6}$ W at 120 GHz.

In summary, we have observed Shapiro steps in the Josephson flux flow state of $\text{Bi}_2\text{Sr}_2\text{CaCu}_2\text{O}_{8+\delta}$ stacked junctions. The position and the magnitude of Shapiro steps in the Josephson flux flow state provide strong evidence of the coherent motion of the Josephson vortex lattice through the whole thickness of the stack in the lowest mode of vortex propagation.

This work was supported by the Japan Science and Technology Corporation, by the Russian State Program on HTS under Grant No. 99016 and by a Grant-in-Aid for Science Research “Novel Quantum Phenomena in Transition-Metal Oxides” from the Ministry of Education, Science, Sports, Culture and Technology of Japan.

-
- [1] R. Kleiner and P. Müller, Phys. Rev. B **49**, 1327 (1994); A. A. Yurgens, Supercond. Sci. Technol. **13**, 85 (2000).
 - [2] L. Balents and L. Radzihovsky, Phys. Rev. Lett. **76**, 3416 (1996); X. Hu and M. Tachiki, *ibid.* **85**, 2577 (2000).
 - [3] L. N. Bulaevskii *et al.*, Phys. Rev. B **53**, 14 601 (1996).
 - [4] T. Koyama and M. Tachiki, Phys. Rev. B **54**, 16 183 (1996).
 - [5] M. Machida *et al.*, Physica (Amsterdam) **330C**, 85 (2000).
 - [6] A. E. Koshelev and I. S. Aranson, Phys. Rev. Lett. **85**, 3938 (2000); cond-mat/0104374.
 - [7] D. A. Ryndyk *et al.*, Phys. Rev. B **64**, 052508 (2001).
 - [8] Y. Matsuda *et al.*, Phys. Rev. Lett. **75**, 4512 (1995); M. B. Gaifullin *et al.*, *ibid.* **83**, 3928 (1999); **84**, 2945 (2000).
 - [9] E. B. Sonin, Phys. Rev. B **63**, 054527 (2001).
 - [10] T. Koyama and M. Tachiki, Solid State Commun. **96**, 367 (1995).
 - [11] J.-U. Lee *et al.*, Appl. Phys. Lett. **67**, 1471 (1995); J.-U. Lee *et al.*, *ibid.* **71**, 1412 (1997).
 - [12] G. Hechtfischer *et al.*, Phys. Rev. B **55**, 14 638 (1997); Phys. Rev. Lett. **79**, 1365 (1997).
 - [13] M. Cirillo *et al.*, Phys. Rev. B **58**, 12 377 (1998).
 - [14] A. V. Ustinov and H. Kohlstedt, Phys. Rev. B **54**, 6111 (1996).
 - [15] S. Sakai *et al.*, Phys. Rev. B **50**, 12 905 (1994); R. Kleiner, Phys. Rev. B **50**, 6919 (1994).
 - [16] Yu. I. Latyshev, S.-J. Kim, and T. Yamashita, IEEE Trans. Appl. Supercond. **9**, 4312 (1999).
 - [17] L. Bulaevskii and J. R. Clem, Phys. Rev. B **44**, 10 234 (1991).